ResearchGate

See discussions, stats, and author profiles for this publication at: https://www.researchgate.net/publication/46099566

Mechanistic study of the phase separation/crystallization process of poly(2-isopropyl-2-oxazoline) in hot water

ARTICLE *in* SOFT MATTER · AUGUST 2010

Impact Factor: 4.03 · DOI: 10.1039/C0SM00114G · Source: OAI

CITATIONS
25

READS
18

8 AUTHORS, INCLUDING:

Peter Cernoch
Institute of Macromolecular Chemistry
28 PUBLICATIONS **229** CITATIONS
SEE PROFILE

Helmut Schlaad
Universität Potsdam
175 PUBLICATIONS **4,419** CITATIONS
SEE PROFILE

Available from: Peter Cernoch
Retrieved on: 27 January 2016

View Online

Mechanistic study of the phase separation/crystallization process of poly(2-isopropyl-2-oxazoline) in hot water†

Christina Diehl,[a] Peter Černoch,[a] Ingrid Zenke,[b] Heike Runge,[b] Rona Pitschke,[a] Jürgen Hartmann,[a] Brigitte Tiersch[c] and Helmut Schlaad*[a]

Received 16th March 2010, Accepted 22nd May 2010
DOI: 10.1039/c0sm00114g

The kinetics of the crystallization of thermoresponsive poly(2-isopropyl-2-oxazoline) in water and the time-dependent evolution of the morphology were examined using wide-angle X-ray scattering and conventional and cryogenic scanning electron microscopy. Results indicate that a temperature-induced phase separation produces a bicontinuous polymer network-like structure, which with the onset of crystallization collapses into individual particles (1–2 μm in diameter) composed of a porous fiber mesh. Nanofibers then preferentially form at the particle surface, thus wrapping the microspheres like a ball of wool. The particle morphology is severely affected by changes in temperature and less by the initial polymer concentration.

Published on 16 June 2010 on http://pubs.rsc.org | doi:10.1039/C0SM00114G
Downloaded by MAX PLANCK INSTITUT FUR KOLLOID on 20 August 2010

Introduction

The crystallization of proteins and of polymers in solution can be induced by liquid–liquid phase separation, for instance, *via* a change in temperature or the addition of salt (salting out). Phase separation increases the local density of crystallizable macromolecules leading to supersaturation.[1] Additionally, concentration fluctuations are generated which enhance the rate of crystal nucleation.[2,3] In several studies, transformation from protein-rich droplets to spherulites has been observed and phase diagrams have been determined to find optimal conditions for crystal growth.[4–6]

Crystallizations of polyethylene,[7] isotactic polypropylene[8] and polystyrene[9] in poor solvent also proceeded *via* this two-step mechanism. Phase separation was induced by quenching a semi-dilute polymer solution below the upper critical solution temperature. Either homogeneous or heterogeneous crystallization occurred in the polymer-rich phase, resulting in the formation of micrometer-sized globules of irregular shape. Also, porous polyamide microspheres were obtained by phase separation, induced by addition of a non-solvent, and subsequent slow crystallization.[10]

Recently, a similar process of phase separation followed by crystallization in aqueous solution has been found to occur for poly(2-isopropyl-2-oxazoline) (PIPOX).[11–14] PIPOX is a crystallizable polymer[15] exhibiting thermoresponsive solution properties;[16–18] the lower critical solution temperature (LCST) is close to human body temperature (~36 °C). Aqueous liquid–liquid phase separation could be simply achieved by heating above the cloud point temperature (T_{CP}). Long-term annealing of the solution in the two-phase regime led to the precipitation of a crystalline material. Crystallization did not occur at temperatures below T_{CP}, hence phase separation seems to be a precondition for crystallization.

The crystalline precipitate, having a melting point of ~200 °C, consisted of uniform spherical particles measuring about 2 μm in diameter. Individual particles were built of nanofibers (~50 nm in width), thus exhibited structural features on two different length scales. The formation of the nanofibers was assigned to a directional crystallization of PIPOX chains into nanoribbons, driven by non-specific hydrophobic and oriented dipolar interactions, and a subsequent fusion process.[11] However, the mechanism of incorporation of the nanofibers into the monodisperse microspheres remained unclear.

The present contribution deals with the mechanism of PIPOX crystallization in water and time-resolved evolution of the particle morphology. Annealing temperature and initial polymer concentration were varied systematically, and the results of crystallization experiments were analyzed using wide-angle X-ray scattering (WAXS) and conventional and cryogenic scanning electron microscopy (SEM).

Experimental

Chemicals and materials

Two samples of α-methyl-ω-hydroxy-PIPOX with apparent number-average molecular weights of 15.4 and 18.3 kDa, polydispersity index ~1.05, were synthesized as described in the ESI†. H_2O was deionized and sterilized using an SG Ultra Clear UV plus TM purification system (Barsbüttel, Germany). D_2O (99.9% D) was used as received from Sigma-Aldrich.

[a]*Max Planck Institute of Colloids and Interfaces, Colloid Chemistry, Research Campus Golm, 14424 Potsdam, Germany. E-mail: schlaad@mpikg.mpg.de; Fax: +49 (0)331 5679502; Tel: +49 (0)331 5679514*
[b]*Max Planck Institute of Colloids and Interfaces, Biomaterials, Research Campus Golm, 14424 Potsdam, Germany*
[c]*University of Potsdam, Institute of Chemistry, Karl-Liebknecht-Straße 24-25, 14476 Golm, Germany*

† Electronic supplementary information (ESI) available: Details of polymer synthesis and characterization, turbidimetric and gravimetric data, additional WAXS curves and SEM images. See DOI: 10.1039/c0sm00114g

 This journal is © The Royal Society of Chemistry 2010

View Online

Downloaded by MAX PLANCK INSTITUT FUR KOLLOID on 20 August 2010
Published on 16 June 2010 on http://pubs.rsc.org | doi:10.1039/C0SM00114G

Analytical instrumentation and methods

Turbidimetry was conducted with a turbidimetric photometer TP1 (Tepper Analytik, Wiesbaden, Germany); heating/cooling rate was 1 K min^{-1}.

WAXS measurements were conducted on an X-ray powder diffraction system (D8, Bruker AXS) using CuK_α radiation. The freeze-dried samples were grinded in a mortar for homogenization purposes and scanned between $2\theta = 5°$ and 25° at a scan rate of 0.02° min^{-1}. For determination of the degree of crystallinity x_c, the intensities $I(2\theta)$ were quantified by integration of each pattern. The crystallinity of a reference sample, which was annealed for several days and extensively washed to remove amorphous material, was arbitrarily set to $x_c = 1$. All diffraction patterns were fitted to this reference by normalization to the (100) peak at $2\theta = 8.04°$, providing the crystalline portions $I_c(2\theta)$. Crystallinity was then calculated from the integrated intensities using

$$x_c = \int_{5°}^{25°} I_c(2\theta)\,\mathrm{d}\,2\theta \Big/ \int_{5°}^{25°} I(2\theta)\,\mathrm{d}\,2\theta$$

In situ WAXS measurements were conducted with 10 wt% polymer solutions in sealed glass capillaries at 60 °C using a Bruker AXS Nanostar equipped with a 2D detector. The 2D patterns were transformed into a 1D radial average of the scattering intensity.

Conventional SEM was performed on a Gemini Leo 1550 microscope operating at 3 kV. Samples were loaded on carbon-coated stubs and coated by sputtering with Au/Pd alloy prior to imaging.

Cryo-SEM was carried out on a Hitachi S-4800 microscope operating at 2 kV. Hot polymer solutions were shock frozen in melting nitrogen and fractured at −180 °C. After etching for 60 s at −98 °C, the samples were sputtered with Pt in the cryo-preparation chamber (Alto 2500, GATAN) and finally transferred into the microscope.

Results and discussion

First, the thermal behavior of the PIPOX (15.4 kDa) sample in aqueous solution was examined by phototurbidimetry. A solution of 1 wt% PIPOX in water exhibited a cloud point temperature (T_{CP}) ≈ 38 °C, and the transition showed little hysteresis in the heating/cooling cycle (ESI†). The later crystallization studies were therefore performed at a temperature of 60 °C, which is between T_{CP} and the PIPOX bulk glass transition temperature (T_g ≈ 68 °C, ESI†). In order to avoid early sedimentation of crystalline materials, D_2O was used as the solvent instead of H_2O because of higher density; the specific density of PIPOX measured in water is 1.226 g ml^{-1} (ESI†). The cloud point temperature of a 1 wt% solution of PIPOX in D_2O is ~37 °C, and the hysteresis is more pronounced than in H_2O (ESI†).[12] The final morphology of the crystalline samples, however, was not affected by the replacement of the solvent (ESI†).

Kinetics of crystallization

Heating of a 1 wt% PIPOX solution in D_2O above the cloud point turned the initially clear solution into a turbid solution. This phase transition was fully reversible when the solution was kept for only short times (<2 h) above the cloud point temperature. However, an increasing amount of precipitate was observed the longer the time of annealing at 60 °C. By dividing the stock solution into several vials, the quantity of precipitate was determined after different times of annealing; insoluble materials were isolated by centrifugation and dried to constant weight. Gravimetric analysis gave a first impression about the time scale of the crystallization process (Fig. 1a). After an induction period of 3 h, precipitation occurred within a period of 7 h. After 10 h at 60 °C, the amount of insoluble material remained constant. However, the fraction of insoluble material may not directly be correlated with crystallinity because some amorphous polymer could be entrapped in the precipitate.

For a direct monitoring of the evolution of crystallinity with time, *in situ* WAXS measurements were performed on 10 wt% PIPOX solutions in D_2O at 60 °C. The relatively high concentration was chosen for the sake of good signal to noise ratio. Characteristic peaks of crystalline PIPOX[11,15] were detected after several hours (ESI†), confirming that the crystallization truly occurred in hot solution and was not initiated by the quenching of the solution to room temperature or evaporation of the solvent. Unfortunately, quantitative information could not be obtained due to inhomogeneous distribution of crystallization nuclei and slow sedimentation of the material out of the focus of the X-ray beam.

Therefore, WAXS studies were conducted with freeze-dried samples. Aliquots from a hot PIPOX stock solution (1 wt% in D_2O) were taken at different times, shock frozen in liquid nitrogen and directly submitted to freeze-drying (to minimize effects of quenching). The diffraction patterns of the semi-crystalline powders in the interval $2\theta = [5°, 25°]$ revealed the same crystalline reflections as observed in the *in situ* measurement. As expected, the intensity and sharpness of the peaks increased with time (Fig. 1b—right). For quantification, the degree of crystallinity x_c of each pattern was calculated from the integrated intensity (*vide supra*). Notably, x_c is an apparent or relative value calculated by means of a reference sample. However, as can be seen by the plot in Fig. 1b—left, the evolution of crystallinity with time follows qualitatively the same trend as the fraction of insoluble material (Fig. 1a).

Both curves exhibit a sigmoidal shape, and the underlying process can therefore be divided into three steps. The first 3–4 h constitute an induction period, in which only little amounts of insoluble or crystalline material are accumulated. Then, the crystallinity steeply increases until a plateau is reached after 7–8 h. Typically, sigmoidal kinetic curves result from autocatalytic processes and are characteristic of crystallization mechanisms proceeding by nucleation and growth.[19] Crystalline nuclei are formed during the induction period, which then grow linearly at a constant rate. With the depletion of amorphous material, the growth rate ultimately slows down until crystallization stops.

The evolution of the crystallite dimension L with time was calculated based on the (100) peak at $2\theta = 8.04°$ applying the Debye–Scherrer equation (ESI†).[20] After a steady increase within the first ~8 h, values of L were found to stay rather constant at ~30 to 35 nm (corresponding to the width of PIPOX fibers as determined earlier by scanning force microscopy).[11] This finding is in line with the earlier developed structure model, proposing

View Online

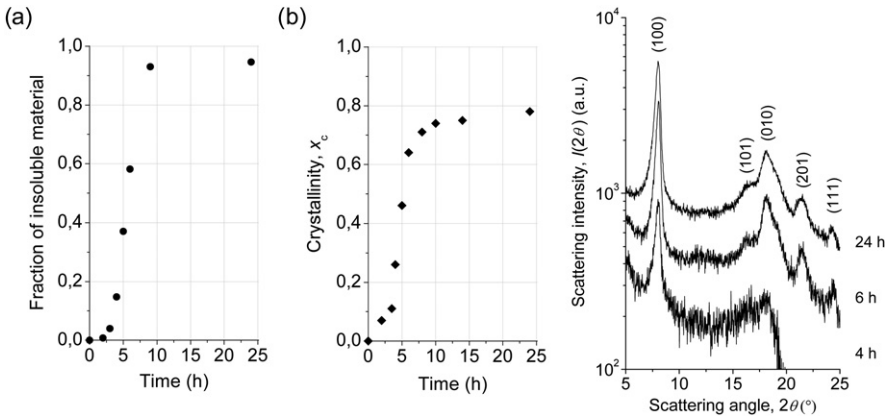

Fig. 1 Time-dependent evolution of (a) the fraction of insoluble material (gravimetric analysis) and (b) the crystallinity of freeze-dried PIPOX precipitate (WAXS), produced during the annealing of a 1 wt% solution of PIPOX in D_2O. Right: exemplary WAXS patterns of PIPOX samples collected at 4, 6, and 24 h; assignment of peaks according to ref. 11.

Downloaded by MAX PLANCK INSTITUT FUR KOLLOID on 20 August 2010
Published on 16 June 2010 on http://pubs.rsc.org | doi:10.1039/C0SM00114G

that the growth of the crystalline PIPOX nanofibers should essentially occur in (010) and not in (100) direction.[11]

Evolution of morphology

In order to elucidate the evolution of the morphology, the freeze-dried PIPOX samples investigated by WAXS were further analyzed by SEM. For reference, the stock solution was heated to 60 °C for just 5 min and immediately freeze-dried. This sample showed no crystalline peaks in WAXS and a similar morphology like the sample collected after 3 h at 60 °C (Fig. 2). The observed droplet-like structure might have been produced by segregation of the polymer upon freezing.

After 4 h, however, the morphology changed considerably, consistent with the appearance of crystalline reflections. SEM showed mostly spherical particles with a diameter of ~2 μm, which are built of a framework of fiber mesh (Fig. 2 and ESI†). With increasing time of annealing and crystallinity of the sample, cavities were filled up with material while the size of the particles remained the same. Rather compact, isolated particles of regular size and shape were obtained after 24 h (ESI†). The newly formed nanofibers appeared to wrap the microspheres, as in a ball of wool, which could be explained by secondary crystallization taking place at the crystal interface. Eventually, as observed in the sample taken at 120 h, crystallization resulted in the formation of clusters consisting of individual particles connected by fibers (Fig. 2 and ESI†). However, the general morphology was maintained at longer times of annealing, and the structure appeared to be stable over time. It is worth being noted that these results could be confirmed in repeat experiments.

In order to clarify the sudden appearance of particles at the onset of crystallization (4 h), the crystallization process in solution was monitored using cryogenic SEM. Samples were taken from hot stock solution (1 wt% PIPOX in D_2O, 60 °C) after 0.5 h, 2 h, and 4 h and shock frozen in melting nitrogen. Surprisingly, the SEM image of the first sample showed a bicontinuous, network-like structure (Fig. 3). Since, according to WAXS experiments, this sample should not contain any crystallized polymer, this network is thought to arise from temperature-induced phase separation into a polymer-poor phase (appearing dark in the image) and a polymer-rich phase (bright). The same morphology could be observed at a higher temperature (70 °C) and in a different solvent (H_2O), but never at a temperature below T_{CP} (data not shown). However, most thermoresponsive polymers, including poly(*N*-isopropylacrylamide) (PNIPAM), collapse into spherical mesoglobules in solution upon heating

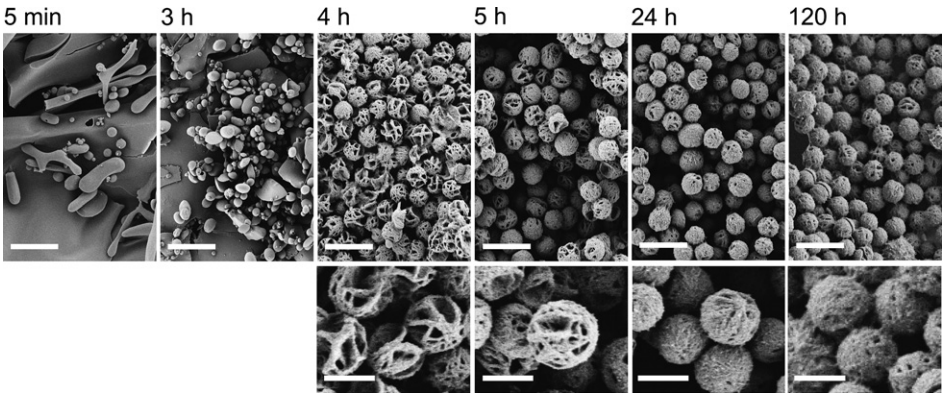

Fig. 2 Scanning electron micrographs of freeze-dried samples produced by annealing of a 1 wt% solution of PIPOX in D_2O at 60 °C for 5 min, 3 h, 4 h, 5 h, 24 h, and 120 h (left to right). Scale bars = 5 μm (top) and 2 μm (bottom).

 This journal is © The Royal Society of Chemistry 2010

View Online

Downloaded by MAX PLANCK INSTITUT FUR KOLLOID on 20 August 2010
Published on 16 June 2010 on http://pubs.rsc.org | doi:10.1039/C0SM00114G

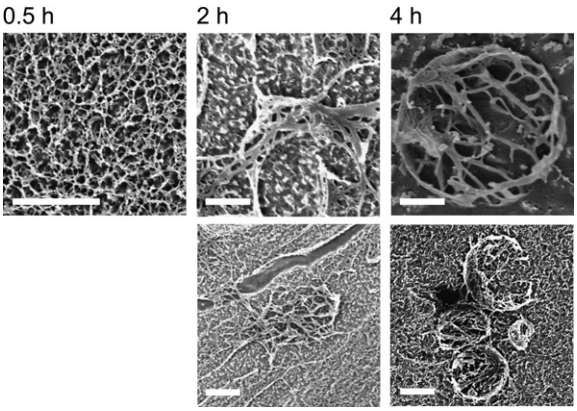

Fig. 3 Cryogenic scanning electron micrographs of a 1 wt% solution of PIPOX in D_2O annealed at 60 °C for 0.5 h, 2 h, and 4 h (left to right). Scale bars = 500 nm (top) and 1 μm (bottom).

above the cloud point temperature.[21] Supported by theoretical calculations, phase separation may also lead to bicontinuous structures, depending on the surface tension and elastic bending modulus of the polymer/solvent interface.[22]

After 2 h at 60 °C, the sample developed inhomogeneities within the network structure or collapsed structures of higher network density (Fig. 3). The collapse of the bicontinuous phase was supposedly induced by crystallization, thus altering both surface tension and bending modulus of the interface. After 4 h, the observed fiber aggregates seemed to bend and ultimately collapse into individual particles of spherical shape (Fig. 3), driven by minimization of interfacial energy. Both particle size and morphology resembled the structures found in the freeze-dried samples after the same time of annealing (*cf.* Fig. 2). The proposed mechanism would particularly explain the formation of hollow hemispheres composed of a fiber mesh. As described above, the porous framework particles may then act as nucleation sites for further crystallization, resulting in porous particles wrapped by a dense layer of nanofibers.

Influence of external parameters

External parameters such as polymer concentration and temperature are expected to have significant impact on the crystallization process, thus giving a handle to control the morphology of PIPOX particles.

The influence of polymer concentration was first examined by comparing samples containing 0.1, 1 and 10 wt% PIPOX (15.4 kDa) in D_2O at 60 °C. Gravimetric analysis revealed that the time-dependent evolution of the fraction of insoluble material was not significantly changed by the variation of polymer concentration (ESI†). Based on thermodynamic considerations, the total amount of polymer in solution affects the mutual fractions of the separated phases but not the weight fractions of polymer in each phase. Accordingly, the crystallization kinetics appear to be independent of polymer concentration. But polymer concentration had severe impact on morphology, as indicated by the SEM images of freeze-dried samples produced by annealing of 0.01, 0.1, and 1 wt% PIPOX (18.3 kDa) in D_2O for 24 h at 50 °C (Fig. 4, left to right). The lower is the concentration the less developed will be the spherical particle morphology (like for

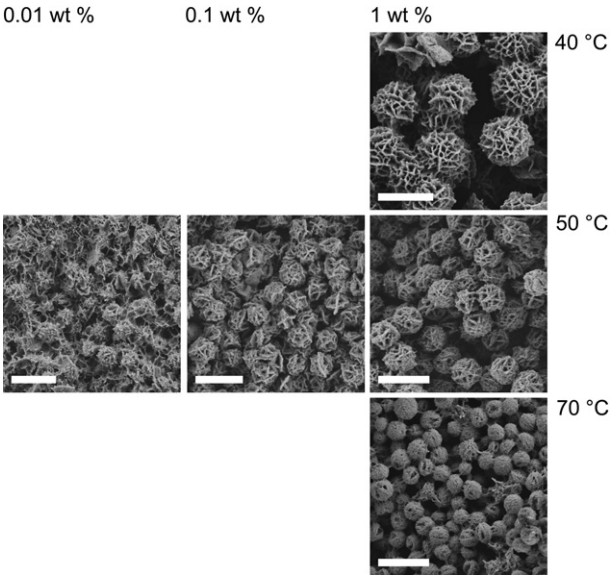

Fig. 4 Scanning electron micrographs of freeze-dried samples produced by annealing of 0.01–1 wt% (left to right) solutions of PIPOX in D_2O for 24 h at 40–70 °C (top to bottom). Scale bars = 5 μm.

short periods of annealing), simply because of lower amounts of available material for crystallization.

The crystallization process significantly slowed down when the temperature of annealing was decreased from 60 °C to 45 °C (gravimetric analysis, ESI†). A drop in temperature affords a decrease of concentration in the polymer-rich phase (*vide supra*), leading to a lower polymer supersaturation and hence nucleation rate. Apart from this thermodynamic issue there is also a kinetic argument, which is slower diffusion of polymer chains at lower temperatures. Regarding morphology, porous particles with a diameter of ~5 μm were obtained at 40 °C (close to T_{CP}), whereas the spheres were considerably smaller and more compact when annealed at 50 °C (~2 to 3 μm) and 70 °C (~1 to 2 μm) (Fig. 4, top to bottom). It is supposed that this effect is due to a change of interfacial properties, *i.e.* surface tension and elastic bending modulus, of the initial network structure. Indeed, the final morphology is also severely altered by the presence of a co-solvent[11] or surfactant[14] (data not shown).

Conclusions

PIPOX is a thermoresponsive (LCST) and also crystallizable polymer. Crystallization occurs in aqueous solution above the cloud point temperature, leading to a slow precipitation of crystalline microparticles. These microparticles have spherical shape and are composed of nanofibers, thus exhibit structural ordering on two different length scales.

Here, the kinetics of the crystallization process and the time-dependent evolution of the morphology were examined using WAXS and conventional/cryogenic SEM. The results indicate that the temperature-induced phase separation of dilute aqueous PIPOX solutions produces a bicontinuous network-like structure (and not mesoglobules). With the onset of crystallization after ~4 h (for 1 wt% PIPOX in D_2O at 60 °C) the network collapses into individual particles composed of a porous fiber mesh. These

View Online

"premature" particles then act, within the next ~5 h, as nucleation sites for secondary crystallization. Nanofibers preferentially form at the particle surface, thus wrapping the microspheres like a ball of wool. This stage is characterized by a steep increase in the crystallinity of the material. Crystallinity reaches a plateau after 8–10 h, that is, when most of the amorphous material is depleted. At this time, rather compact and isolated microspheres of uniform size (~1 to 2 μm in diameter) have been formed. Upon further annealing for several days, the particles get interconnected by nanofibers.

The final morphology can be controlled by changing the crystallization temperature (or by the addition of co-solvents or surfactants), while polymer concentration has only a minor effect (similar to time of annealing). Particles become bigger, up to 5 μm in diameter, and more porous upon lowering the temperature close to the cloud point temperature.

This process provides a simple and "green" route to crystalline, eventually (bio-)functional,[23] microparticles. Such microparticles could be interesting materials for instance for special chromatographic applications. Crystalline PIPOX particles are stable at temperatures up to ~160 °C and pressures up to 250 bar (data not shown). Particles can be redispersed and are stable in water and most organic solvents.

Currently, crystallization studies are extended to thermoresponsive poly(2-alkyl-2-oxazoline)s other than PIPOX.

Acknowledgements

Klaus Tauer, Peter Fratzl, and Markus Antonietti are thanked for very stimulating and helpful discussions. Jessica Brandt, Marlies Gräwert, and Olaf Niemeyer are thanked for helping hands and technical assistance. Financial support was given by Max Planck Society and Fraunhofer Society through the Network of Excellence "Synthetic Bioactive Surfaces".

Notes and references

1 L. F. Filobelo, O. Galkin and P. G. Vekilov, *J. Chem. Phys.*, 2005, **123**, 014904.
2 P. R. t. Wolde and D. Frenkel, *Science*, 1997, **277**, 1975–1978.
3 W. Hu and D. Frenkel, *Macromolecules*, 2004, **37**, 4336–4338.
4 S. Tanaka, M. Yamamoto, K. Ito, R. Hayakawa and M. Ataka, *Phys. Rev. E: Stat. Phys., Plasmas, Fluids, Relat. Interdiscip. Top.*, 1997, **56**, R67–R69.
5 M. Muschol and F. Rosenberger, *J. Chem. Phys.*, 1997, **107**, 1953–1962.
6 C. Haas and J. Drenth, *J. Phys. Chem. B*, 1998, **102**, 4226–4232.
7 P. Schaaf, B. Lotz and J. C. Wittmann, *Polymer*, 1987, **28**, 193–200.
8 H. K. Lee, S. C. Kim and K. Levon, *J. Appl. Polym. Sci.*, 1998, **70**, 849–857.
9 J. H. Aubert, *Macromolecules*, 1988, **21**, 3468–3473.
10 Y. Asano, N. Kimio and S. Yao, *J. Appl. Polym. Sci.*, 2003, **90**, 2428–2432.
11 A. L. Demirel, M. Meyer and H. Schlaad, *Angew. Chem., Int. Ed.*, 2007, **46**, 8622–8624.
12 R. Obeid, F. Tanaka and F. M. Winnik, *Macromolecules*, 2009, **42**, 5818–5828.
13 N. Morimoto, R. Obeid, S. Yamane, F. M. Winnik and K. Akiyoshi, *Soft Matter*, 2009, **5**, 1597–1600.
14 H. Schlaad, C. Diehl, A. Gress, M. Meyer, A. L. Demirel, Y. Nur and A. Bertin, *Macromol. Rapid Commun.*, 2010, **31**, 511–525.
15 M. Litt, F. Rahl and L. G. Roldan, *J. Polym. Sci., Part A2*, 1969, **7**, 463–473.
16 H. Uyama and S. Kobayashi, *Chem. Lett.*, 1992, 1643–1646.
17 C. Diab, Y. Akiyama, K. Kataoka and F. M. Winnik, *Macromolecules*, 2004, **37**, 2556–2562.
18 M. Meyer, M. Antonietti and H. Schlaad, *Soft Matter*, 2007, **3**, 430–431.
19 L. Mandelkern, *Biophys. Chem.*, 2004, **112**, 109–116.
20 A. L. Patterson, *Phys. Rev. E: Stat. Phys., Plasmas, Fluids, Relat. Interdiscip. Top.*, 1939, **56**, 978–982.
21 V. Aseyev, S. Hietala, A. Laukkanen, M. Nuopponen, O. Confortini, F. E. Du Prez and H. Tenhu, *Polymer*, 2005, **46**, 7118–7131.
22 E. A. Maresov and A. N. Semenov, *Macromolecules*, 2008, **41**, 9439–9457.
23 C. Diehl and H. Schlaad, *Chem.–Eur. J.*, 2009, **15**, 11469–11472.

Downloaded by MAX PLANCK INSTITUT FUR KOLLOID on 20 August 2010
Published on 16 June 2010 on http://pubs.rsc.org | doi:10.1039/C0SM00114G

 This journal is © The Royal Society of Chemistry 2010